A modelling strategy for enhanced recovery strength and tailorable shape transition behavior in shape memory copolymer

Xiaodong Wang,[†] Jian Wei, [‡] Haibao Lu[*,†], Denvid Lau[*,‡] and Yong-Qing Fu[§]

[†]Science and Technology on Advanced Composites in Special Environments Laboratory, Harbin Institute of Technology, Harbin 150080, China

[‡]Department of Architecture and Civil Engineering, City University of Hong Kong, Tat Chee Avenue, Kowloon, Hong Kong

[§]Faculty of Engineering and Environment, University of Northumbria, Newcastle upon Tyne, NE1 8ST, UK

[*]Corresponding author, E-mail: luhb@hit.edu.cn and denvid.lau@cityu.edu.hk

Abstract: By integrating Fox-Flory equation and rubber elasticity principle, a phenomenologically constitutive model was proposed in this study to describe high mechanical recovery strength and tailorable shape transition behavior of shape memory polymer (SMP) copolymers. Thermodynamics of different monomers in the copolymers were formulated by considering their influences on glass transition temperatures (T_g) and elastic moduli based on the Fox-Flory and Gordon-Taylor equations. Effects of T_g, fraction, molecular weight, storage modulus and rubbery modulus of various monomers on thermomechanical and shape recovery behaviors of the SMP copolymers were theoretically investigated and discussed. Working principles of enhanced mechanical strength and tailorable shape transition behavior of the SMP copolymers have been well described using this newly proposed model, which offers an effective strategy for designing SMPs with high mechanical strength

and desirable shape memory behavior. Furthermore, molecular dynamics simulations were used to predict the glass transition temperature from a molecular scale and the results were fit well with our modelling results.

Keywords: shape memory copolymers, recovery strength, shape transition behavior

1. Introduction

Shape memory polymers (SMPs) are one of the key stimuli-responsive materials with the ability to regain their permanent shape from a temporary one in presence of the external stimuli, including heat [1,2], solvent [3,4], light [5], electrical and magnetic field [6,7]. This feature is defined as shape memory effect (SME), which has found a myriad of practical applications in biomedical devices [8,9], aerospace deployable and periodic structures [10,11], sensors and actuators [12]. In comparisons with the conventional shape memory alloys and ceramics, SMPs present many unique advantages, such as large recovery strain, low cost and simple manufacturing process [13-16]. However, their relatively low recovery strengths severely limit their practical and potential applications [17].

To overcome this issue, fiber reinforced SMP composites [18] and high enthalpy SMPs [19] have been made and their rubbery moduli can be as high as 17-20 MPa. However, their shape recovery performance is often undesirable because it is difficult to control the rearrangements of macromolecules at the molecular scale. Therefore, photo-polymerized SMP copolymers, i.e., MMA-co-PEGDMA (methyl methacrylate (MMA) and poly(ethylene glycol) dimethacrylate (PEGDMA)) [20,21] and

tBA-co-PEGDMA (*tert*-Butyl acrylate (tBA) and poly(ethylene glycol) dimethacrylate (PEGDMA)) [22,23], were synthesized in order to achieve both good mechanical recovery strengths and tailorable glass transition temperatures (T_g) by controlling weight fraction and molecular weight of the PEGDMA monomers.

Recently, several theoretical models have been proposed to describe the working mechanism and shape memory behaviors of SMPs. For example, Liu et al. formulated a model by combining phase transition theory and viscoelasticity in order to characterize the viscoelastic properties at different pre-strains [24]. Furthermore, the working mechanisms of temperature- and time-dependent SMEs in SMPs have been well predicted and described using their proposed models [25,26]. On the other hand, structural relaxation [27], multi-SME [28] and thermochemically SME [29] have also been well investigated using multi-branche models. However, it is critically needed to develop theoretical models to describe the working mechanisms of these SMP copolymers with high mechanical recovery strengths.

This paper will develop a phenomenological model for the unique characteristics of the SMP copolymers with high mechanical recovery strength and tailorable shape transition behavior. The stored mechanical energy is initially obtained and used to link with the high recovery strength in SMP copolymers [30]. Fox-Flory equation [31] and Gordon-Taylor [32] equation are then combined to characterize the effects of molecular weight and weight fraction of PEGDMA monomer on T_g of the SMP copolymer. Furthermore, rubbery elasticity theory [27] is then employed to formulate a thermomechanically constitutive model to investigate the fundamental working

mechanism of SMP copolymers with their high mechanical recovery strengths. Finally, both the Weibull statistics model [34] and phase transition theory [35] are used to investigate the tailorable shape recovery behaviors of the SMP copolymers. The simulation results have been compared with the experimental ones in order to verify the proposed model.

2. Modelling of mechanical recovery strength

Mechanical recovery stress is the driving force for the shape recovery of the SMPs in their rubbery states. This stress is originated from the release of stored mechanical energy in the pre-loading and deformation process [1]. When the SMPs are heated to above their transition temperature, the stored mechanical energy and stress are therefore released from the SMPs [19-23]. Here, the mechanical recovery strength is used to link with the recovery stress and rubbery modulus in the shape recovery process of SMP copolymer.

Glass transition temperature ($T_g(s)$) of PEGDMA monomer as a function of the molecular weight (M_n) in the MMA-co-PEGDMA copolymer can be obtained according to the Fox-Flory equation [31] as follows:

$$T_g(s) = T_{g\infty}(s) - \frac{k_g}{M_n} \tag{1}$$

where $T_{g\infty}(s)$ is the glass transition temperature of the PEGDMA monomer while the molecular weight is infinity, and k_g is a given parameter.

The T_g of the SMP copolymer can be determined by those of PEGDMA and MMA monomers, and is ruled by the Gordon-Taylor equation [32]:

$$T_g = \frac{T_g(h) + \left(KT_g(s) - T_g(h)\right)W_s}{1 + (K-1)W_s} \tag{2}$$

where $T_g(h)$ is the glass transition temperature of the MMA monomer in the SMP copolymer, W_s is the weight fraction of PEGDMA and K is a Gordon-Taylor constant.

Combining equations (1) and (2), we can obtain the T_g of SMP copolymer as a function of the weight fraction of PEGDMA monomer:

$$T_g = \frac{T_g(h) + \left(KT_{g\infty}(s) - K\frac{k_g}{M_n} - T_g(h) \right)W_s}{1 + (K-1)W_s} \tag{3}$$

Calculation results using equation (3) are plotted in Figure 1, which is also compared with experiment data of MMA-co-PEGDMA polymer network reported in Ref. [20]. The parameter values of equation (3) are presented in Table 1. It is found that the T_g value is gradually increased with the decrease of M_n at the given weight fraction of the PEGDMA monomer. On the other hand, the weight fraction of PEGDMA also shows a critical influence on the T_g value of SMP copolymer, which is gradually decreased with an increase in weight fraction of the PEGDMA monomer. Combining the influences of the above two parameters, it is found that the decrease rate of T_g is much smaller with the increase of the weight fraction of PEGDMA when the molecular weight of PEGDMA monomer, M_n, is small, for example $M_n = 330$. Based on equation (3), the fundamental requirements for this behavior are: (1) the T_g value of PEGDMA should be larger when the value of M_n is smaller; and the T_g value of PEGDMA should be close to that of the MMA. Therefore, in these cases, the change in the weight fraction of PEGDMA has little influence on the

T_g of SMP copolymer. Practically, we can use the molecular design to change T_g values of the SMP copolymer.

Table 1. Parameter values used in equations (3) and (9).

E_{hs} (MPa)	$\alpha\rho\,(g/cm^3)$	$T_g(h)(K)$	K	$T_{g\infty}$(s)(K)	k_g	$\theta(K)$
2.1	5.57	414.89	1.10	159.97	-7.7×10^4	15

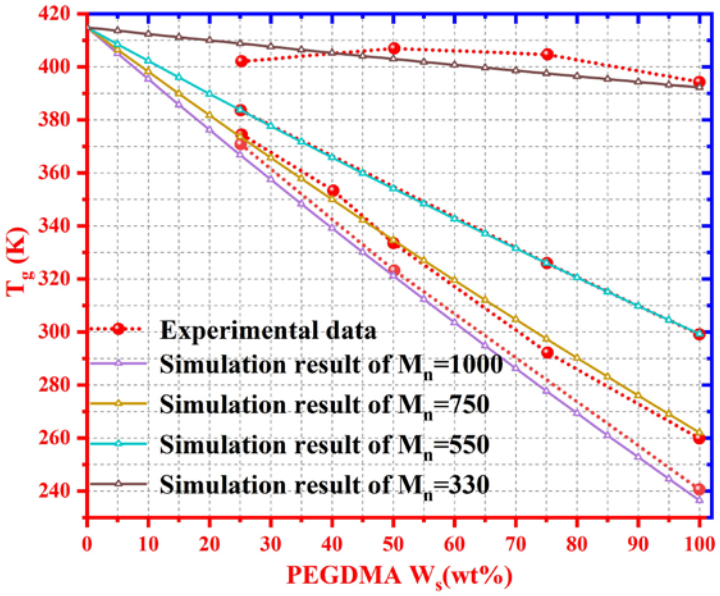

Figure 1. Comparisons between numerical results using equation (3) and experimental data of the MMA-co-PEGDMA [20] at given molecular weights of PEGDMA monomer, e.g., M_n=330, 550, 750 and 1000.

Meanwhile, the stored mechanical energy in the MMA-co-PEGDMA SMP copolymer is released when the SMP is heated above its T_g, thus triggering the shape recovery. Therefore, the recovery strength of SMP copolymer is determined by its rubbery modulus [30]. Here, effects of weight fraction (W_s) and copolymer molecular weight (M_n) of PEGDMA monomer on the rubbery modulus of the SMP copolymer

(E_r) should be studied in order to identify their constitutive relationships with the mechanical recovery strength. For MMA-co-PEGDMA molecules, their rubbery modulus is incorporated into the MMA and PEGDMA monomers in a series-connection to resist to an external loading, which can be described using:

$$E_r = E_{hs}(1-W_s) + E_s W_s \tag{4}$$

where E_{hs} and E_s are the rubbery moduli of the MMA and PEGDMA monomers, respectively. The rubbery modulus of the MMA monomer is assumed a constant because the molecular weight is kept a constant. Therefore, the rubbery modulus of the SMP copolymer is determined by the PEGDMA monomer with a variety of molecular weights (M_n). Based on the rubbery elasticity theory [33], the rubbery modulus of PEGDMA (E_s) is given by:

$$E_s = 3N_s RT \tag{5}$$

where R is gas constant (R =8.314J/(mol · K)) and T is the temperature of polymers in their rubber states. N_s (with a unit of mol/cm^3) is defined as molar number of the crosslinking points of PEGDMA monomer (n_s) per cubic centimeter and n_s is set as α times of the molar number of monomer. We can further obtain the following equation:

$$N_s = n_s / V = \frac{\alpha m W_s}{M_n} / V = \frac{\alpha \rho W_s}{M_n} \tag{6}$$

where ρ is the density, m is the weight and V is the volume of the SMP copolymer.

We assume that the rubber state is dominant when the temperature (T) is higher than T_g and their temperature difference is θ (K). Therefore, we can further rewrite

equation (3) as:

$$T = \frac{T_g(h) + \left(KT_{g\infty}(s) - K\frac{k_g}{M_n} - T_g(h) \right) W_s}{1 + (K-1)W_s} + \theta \tag{7}$$

By substituting equations (6) and (7) into equation (5), we can obtain:

$$E_s = 3N_s RT = \frac{3\alpha\rho RW_s}{M_n} \left[\frac{T_g(h) + \left(KT_{g\infty}(s) - K\frac{k_g}{M_n} - T_g(h) \right) W_s}{1 + (K-1)W_s} + \theta \right] \tag{8}$$

Combining equation (8) with (4), we can obtain the expression of the rubbery modulus (E_r) as a function of the weight fraction (W_s) and the molecular weight (M_n) of the PEGDMA as follows:

$$E_r = E_{hs}(1 - W_s) + \frac{3\alpha\rho RW_s^{\,2}}{M_n} \left[\frac{T_g(h) + \left(KT_{g\infty}(s) - K\frac{k_g}{M_n} - T_g(h) \right) W_s}{1 + (K-1)W_s} + \theta \right] \tag{9}$$

To verify the equation (9), simulation results based on the proposed model were plotted and then compared with the experimental data reported in Ref. [20], and the results are shown in Figure 2. During analysis, both the weight fraction and molecular weight of the PEGDMA are varied in order to study their effects on the rubbery modulus of SMP copolymer. The obtained fitting data are presented in Table 1. It is found that the rubbery modulus is increased with an increase in the weight fraction (or decrease in the molecular weight) of the PEGDMA monomer. Clearly these simulation results are slightly larger than those of the experimental ones because during experiments the MMA and PEGDMA monomers in a series connection will resist an external loading. Indeed, the connection modes of the MMA and PEGDMA

monomers are complex in the SMP copolymer. With different types of connection modes, the contributions of the MMA and PEGDMA monomers to the rubbery modulus of the SMP copolymer are quite different, thus causing the differences between the simulation result (of series connection mode) with the experimental data, as shown in Figure 2.

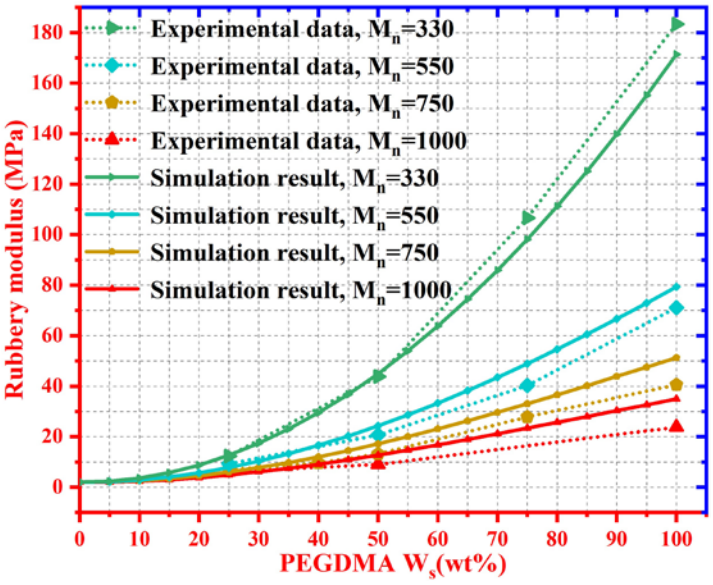

Figure 2. Comparisons between results obtained from equation (9) and experimental data of the rubbery modulus as a function of W_s and M_n [20].

Molecular dynamics (MD) simulation is further used to predict the glass transition temperature with respect to the change of the weight fraction of the PEGDMA monomer. MD approach has been used in literature to predict the *T*g of polymer systems and the results agreed well with the experimental findings [36,37]. The atomistic models of the MMA monomer and PEGDMA crosslinkers, and the copolymer systems with the corresponding weight fractions of PEGDMA (W_s=20%, 40%, 60% and 80%) are constructed as shown in Figure 3. The interactions in the

polymer systems are described by the consistent valence force field (CVFF) [38]. The partial charges of different types of atoms are calculated using the bond increment method [39]. The non-bonded interactions, including van der Waals and Coulombic interactions, are calculated with a cutoff of 10Å. The particle-particle and particle-mesh solver is used to account for the long-range Coulombic interaction [40]. The time step of 1 fs is used in MD simulations. Periodic boundary conditions are applied to all the directions. The original polymer structures are first equilibrated at a temperature of 450 K and a pressure of 1 atm under the *NPT* ensemble (constant particle number (*N*), constant pressure (*P*) and constant temperature (*T*)) for 1 ns. Then the systems are gradually cooled down to 250 K at a step of 1×10^{10} K s^{-1}. All the MD simulations are carried out using a large-scale atomic/molecular massively parallel simulator (LAMMPS) [41].

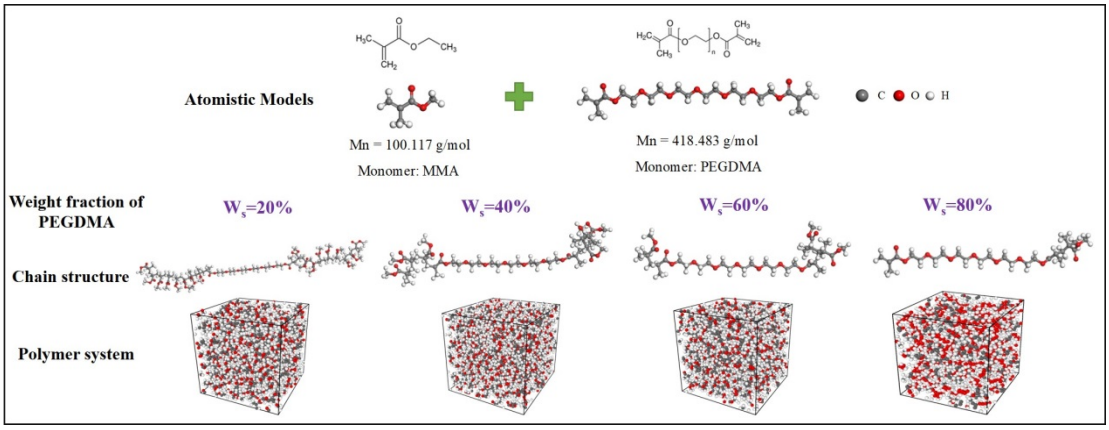

Figure 3. The molecular sketch map of the MMA, PEGDMA monomer, and the polymer system at the weight fraction of PEGDMA (W_s=20%, 40%, 60% and 80%), respectively.

Figure 4 shows the T_g values obtained from the intersections of the two linear

fittings of the glassy and rubbery regions in the plots. We can obtain that T_g=393.5 K for the case of W_s=20%; T_g=381.4 K for the case of W_s=40%; T_g=364.3 K for the case of W_s=60%; and T_g=357.6 K for the case of W_s=80%. All of these are close to the modelling results of T_g=399.59 K, 384.88 K, 370.73K and 358.54K obtained using equation (3). This indicates clearly that the prediction of the T_g from the molecular scale is applicable.

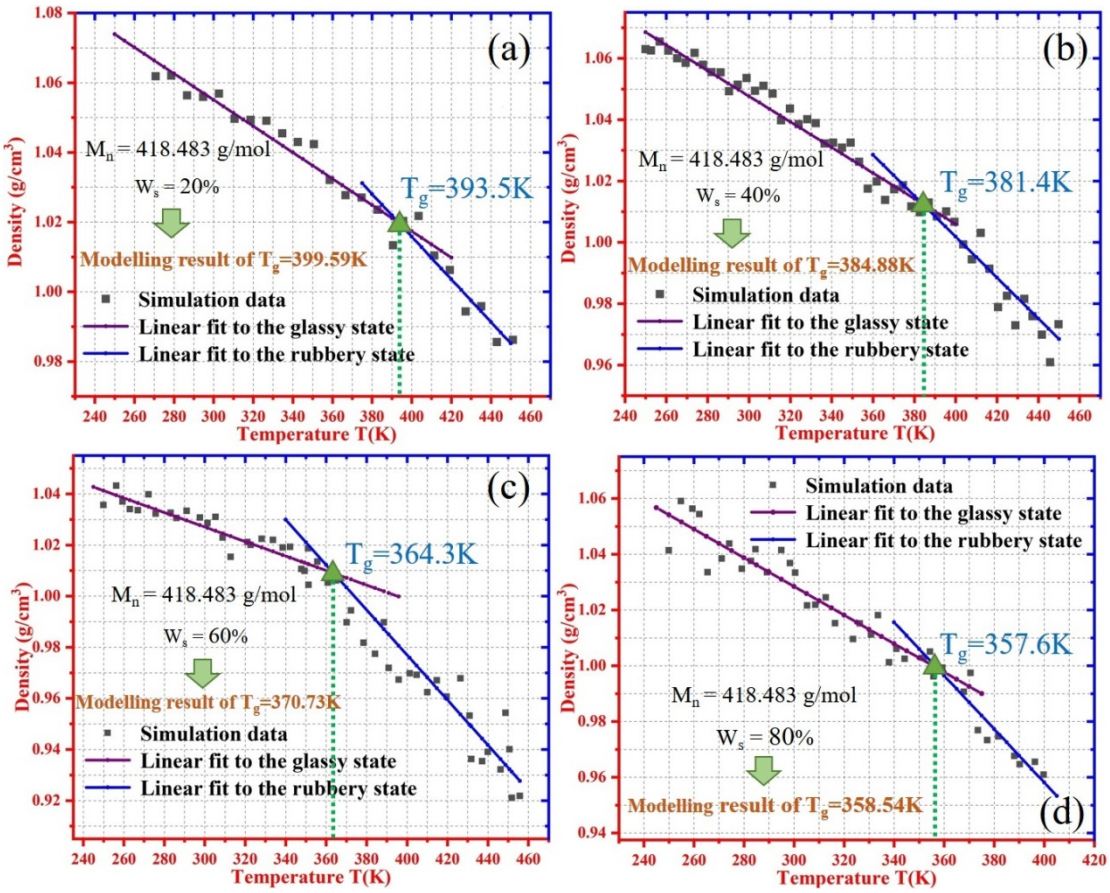

Figure 4. Calculated value of T_g from the intersections of the two linear fits to the glassy and rubbery regions at (a) W_s=20%; (b) W_s=40%; (c) W_s=60% and (d) W_s =80%.

Furthermore, equation (9) provides an effective model to tailor and design the values of T_g and E_r of the SMP copolymer by control of weight fraction and

molecular weight of the monomers. The simulation results based on the proposed model (equation (9)) are presented in Figure 5. As revealed in Figure 5(a), the T_g of SMP copolymer is essentially determined by the molecular weight (M_n) of the monomer. It is also found that the T_g is gradually increased with an increase in the weight fraction (W_s) when M_n=200 (M_n<300). Whereas it is gradually decreased with an increase in the weight fraction (W_s) of PEGDMA monomer when M_n=400, 500, 600 or 700 (e.g., $M_n > 300$). At a given weight fraction (e.g., W_s=100%), the T_g values are decreased from 543.4ºC to 269.4ºC when the molecular weight (M_n) is increased from 200 to 700. Effects of weight fraction and molecular weight of the PEGDMA monomer on the rubbery modulus have been further studied, and the results are shown in Figure 5(b). The rubbery modulus is found to increase with the weight fraction (W_s), and to reach its highest value when W_s=100%. They are 56.4 MPa, 91.2 MPa, 127.3 MPa, 199.3 MPa to 387.7MPa when the molecular weights are M_n=700, M_n=600, M_n=500, M_n=400, M_n=300 to M_n=200, respectively. For the SMP copolymer, its shape recovery will occur when it is heated above its T_g. This means that the shape recovery process is induced when the SMP is in its rubbery state. Therefore, the mechanical recovery strength of the SMP copolymer is mainly determined by the rubbery modulus. The above simulation results reveal that the rubbery modulus can be significantly increased by decreasing the molecular weight (M_n) or increasing the weight fraction (W_s) of the PEGDMA monomer, thus increasing the mechanical recovery strength.

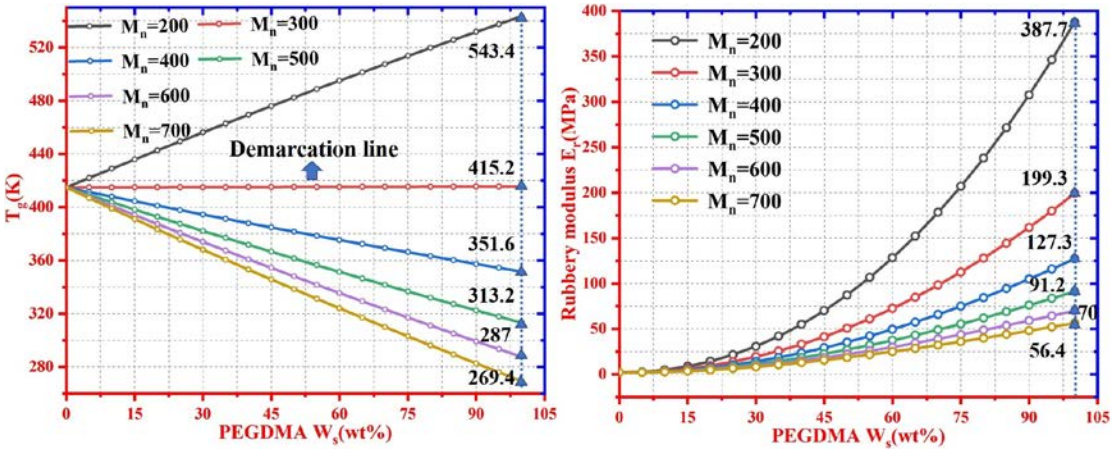

Figure 5. Simulation results of T_g and E_r as a function of molecular weight (M_n) and weight fraction (W_s) of PEGDMA in SMP copolymer.

Weibull statistical model [34] is further introduced to characterize the storage modulus which is a critical parameter to determine the rubbery modulus. The constitutive relationship for storage modulus ($E(T)$) is given by [34]:

$$E(T) = (E_1 - E_2)\cdot\exp\left(-\left(\frac{T}{T_\beta}\right)^{m_1}\right) + (E_2 - E_r)\cdot\exp\left(-\left(\frac{T}{T_g}\right)^{m_2}\right) + E_r\cdot\exp\left(-\left(\frac{T}{T_f}\right)^{m_3}\right) \quad (10)$$

where T_β is the transition temperature of β relaxation in the monomer, T_f is the flow temperature of the polymer chains and m_i is Weibull moduli. Both E_1 and E_2 are the stiffness values of the MMA and PEGDMA monomers in the SMP copolymer, respectively.

According to the equation (10), a constitutive relationship among the storage modulus ($E(T)$), temperature (T), glass transition temperature (T_g) and rubbery modulus (E_r) can be obtained:

$$E(T) = (E_2 - E_r)\cdot\exp\left(-\left(\frac{T}{T_g}\right)^{m_2}\right) + E_r \quad (11)$$

By substituting equations (3) and (9) into equation (11), the influences of weight

fraction and molecular weight of PEGDMA monomer on the storage modulus of SMP copolymer can be obtained:

$$\begin{cases} T = \dfrac{T_g(h) + \left(KT_{g\infty}(s) - K\dfrac{k_g}{M_n} - T_g(h) \right) W_s}{1 + (K-1)W_s} + \theta \\ E_r = E_{hs}(1 - W_s) + \dfrac{3\alpha\rho R W_s^{\,2}}{M_n} \left[\dfrac{T_g(h) + \left(KT_{g\infty}(s) - K\dfrac{k_g}{M_n} - T_g(h) \right) W_s}{1 + (K-1)W_s} + \theta \right] \\ \Downarrow\Downarrow\Downarrow \\ E(T) = (E_2 - E_r) \cdot \exp\left(-\left(\dfrac{T}{T_g} \right)^{m_2} \right) + E_r \end{cases} \quad (12)$$

Table 2. Experimental data of tBA-co-PEGDMA copolymers in Ref. [22].

M_n=550	E_r (MPa)	2.4	5.2	12.8	67.5
	T_g (K)	280	306	312	322
	W_s	10%	20%	40%	100%
M_n=750	E_r (MPa)	1.6	3.08	7.2	38.2
	T_g (K)	242	278	298	313
	W_s	10%	20%	40%	100%

Figure 6(a) provides the numerical results of the rubbery moduli as a function of the weight fraction of PEGDMA monomer with different molecular weights of M_n =550 and 750 for the SMP copolymer. The experimental data of the tBA-co-PEGDMA copolymer reported in ref. [22] are also plotted in Figure 6(a) for comparisons. Tables 2 and 3 list the experimental data [22] and the fitted data used in

equation (12), respectively. It is found that the simulation results are in good agreements with the experimental ones. With the molecular weight increased from 550 to 750, the rubbery modulus of the SMP copolymer is increased from 7.2 MPa to 12.8 MPa at a given weight fraction of W_s=40%. It confirms that the rubbery modulus of the tBA-co-PEGDMA copolymer is strongly determined by the molecular weight of PEGDMA monomer.

Table 3. Parameter values used in equation (12).

E_h(MPa)	$\alpha\rho\,(g/cm^3)$	$T_g(h)(K)$	K	$T_{g\infty}$(s)(K)	k_g	$\theta(K)$	m_2
1.23	5.95 (4.55)	339.87	1.882	233.18	-58.72	15	23.21

Figures 6(b) and 6(c) plot the numerical results of the storage moduli as a function of temperature for the SMP copolymer with molecular weight of PEGDMA monomer M_n=550 and 750, respectively. The experimental data obtained from ref. [22] of the tBA-co-PEGDMA are also collected and plotted for comparisons. At a given weight fraction and a given T_g, the numerical results obtained from the theoretical model fit well with the experimental results. The storage modulus is mainly determined by the molecular weight, weight fraction and T_g of the PEGDMA monomer in the tBA-co-PEGDMA copolymer. In other words, the storage modulus of the SMP copolymer can be tailored and designed through adjusting the molecular weight, weight fraction and T_g of the monomers inside.

Taking tBA-co-PEGDMA for example, this SMP copolymer is incorporated from two monomers, i.e. PEGDMA and tBA monomers. There are definite differences in

the T_g and thermomechanical properties between the PEGDMA and tBA monomers. With an increase in the molecular weight or weight fraction of the PEGDMA monomer, the T_g and thermomechanical properties of the tBA-co-PEGDMA copolymer are decreased. Therefore, the T_g and thermomechanical properties of the tBA-co-PEGDMA copolymer can be tailored and designed through adjusting the molecular weight and weight fraction of the PEGDMA monomer. Meanwhile, other types of monomers can also be selected, but not the PEGDMA monomer, in order to tailor and design the SMP copolymer based on the different T_g and thermomechanical properties of the monomers.

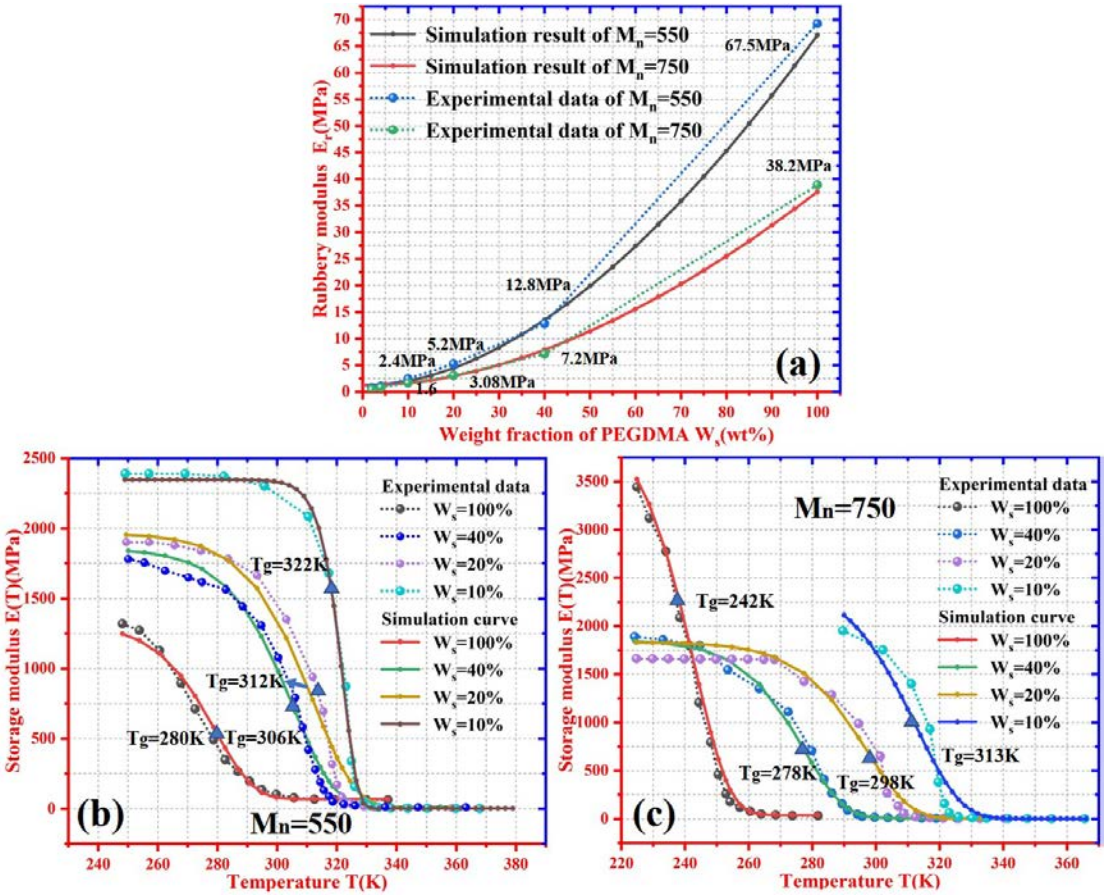

Figure 6. (a) Comparisons between simulation results and experimental data [22] of the rubbery modulus as a function of weight fraction. (b) and (c) Comparisons

between simulation results and experimental data of the storage modulus of the SMP copolymers with molecular weight of M_n=550 and M_n=750, respectively [22].

3. Modelling of shape transition behavior

Based on phase transition theory [29], volume fraction ratio of a frozen phase (ϕ_f) is equal to the normalized unrecovered strain. Therefore, the constitutive relationship between the recovery strain ($\varepsilon(T)$) and frozen phase ϕ_f can be written as [35]:

$$\varepsilon(T)/\varepsilon_{pre} = 1-\phi_f = 1/(1+c_f(T_h - T)^n) \tag{13}$$

where c_f and n are material constants. T_h is the transition temperature and ε_{pre} presents the pre-deformed strain. As is well known, phase transition model is generally limited to the case with a small strain (<10%) [24,26], which the non-linearity of rubbery elasticity of polymer is often ignored. It should be noted that the SMP presents a viscoelastic shape deformation with a strain larger than 10%. Here the phase transition model is employed to characterize the shape recovery behavior where the strain of SMP is larger than 10%. On the other hand, the phase transition model should be combined with the viscoelasticity of SMP in order to characterize the large deformation behavior under the tensile loading (e.g., the strain is larger than 10%) [24,26].

Based on equation (13), the recovery strain is determined by the transition temperature (T_h) which is mainly determined by the T_g. Here, we set $T_h = T_g + \theta'$ (θ' is the difference between T_h and T_g) and equation (13) is therefore rewritten as:

$$\varepsilon(T)/\varepsilon_{pre} = 1-\phi_f = 1/(1+c_f(T_g+\theta^{'}-T)^n) \quad (14)$$

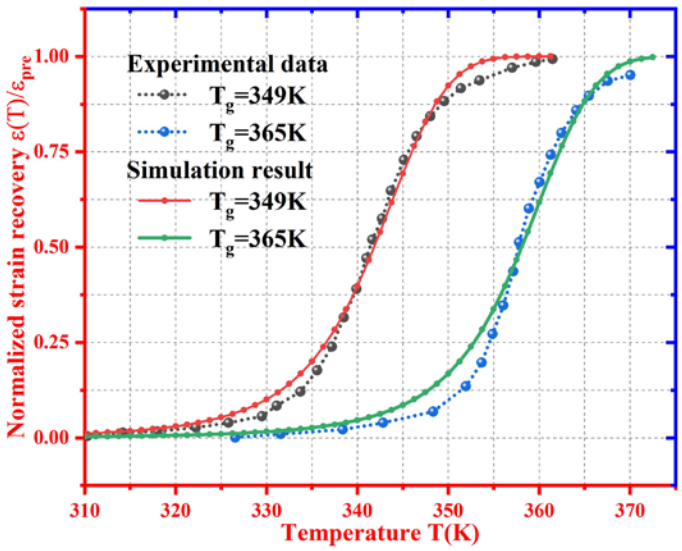

Figure 7. Comparisons between the numerical results obtained from equation (14) with experimental data [20] of the free recovery strain.

Equation (15) is then employed to predict the free recovery process of the MMA-co-PEGDMA copolymer with T_g=349 K and 365 K [20], which have been reported in ref. [20]. The obtained simulation results are c_f =4.01×10^{-8}, n=4.64 and $\theta^{'}=12.71K$. As shown in Figure 7, the simulation results of the free recovery strain as a function of temperature fit well with experimental data obtained using the same parameters [20]. The proposed model shown in equation (14) has therefore been verified by the experimental results and provides an effective approach to predict the free shape recovery of the MMA-co-PEGDMA copolymer.

Combining equations (3) with (14), the effects of the molecular weight and weight fraction on the free recovery strains are further investigated by using M_n=300 (400, 500, 600 or 700) and $W_s = 0.8$. As presented in Figure 8(a), the obtained results show that the free recovery curves are gradually shifted to higher temperature side, e.g.,

from 309K, 322K, 345K, 375.3K to 429.5K, with an increase in the molecular weight M_n from 300 g/mol, 400 g/mol, 500 g/mol, 600 g/mol to 700 g/mol, at a given weight fraction of PEGDMA monomer $W_s = 0.8$. On the other hand, the numerical results shown in Figure 8(b) reveal that the free recovery curves are gradually shifted to the higher temperature side from 324.2K, 346.7K, 362K, 382K to 402.3K with a decrease in the weight fraction of W_s=1.0, 0.8, 0.6, 0.4 to 0.2. These simulation results clearly show the significant effects of both the molecular weight and weight fraction of the PEGDMA monomer on the free recovery strain of MMA-co-PEGDMA copolymer. The tailorable shape recovery behavior is originated from the effects of molecular weight and weight fraction on the T_g of the SMP copolymer. With an increase in the T_g, the free recovery strain is induced at a higher temperature as shown in Figure 8. These simulation results verify that the proposed model in the equation (14) provides an effective and critical approach to design the T_g of the SMP copolymer in order to achieve its tailorable shape transition behavior.

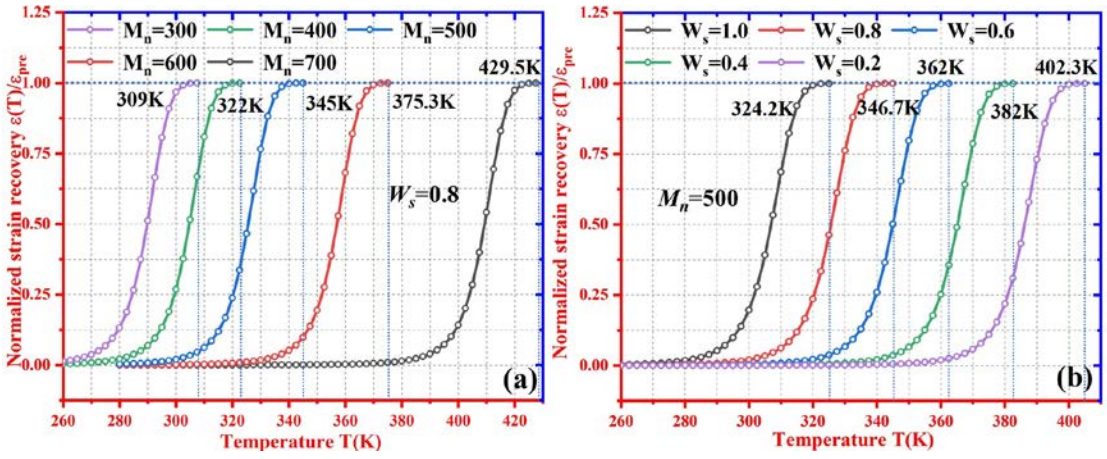

Figure 8. Numerical results of the normalized strain recovery as a function of temperature at a given weight fraction of W_s=0.8 (a) and (b) at a given molecular weight of M_n=500.

To further investigate the mechanical recovery strength, it is necessary to study the shape recovery stress of the SMP copolymer. In certain applications, the recovery stress is often used to estimate the actuation capability of the shape memory polymers [35,36]. According to equations (11) and (14), the recovery stress as a function of rubbery modulus (E_r) and T_g can be written as:

$$\sigma(T) = E(T) \cdot \varepsilon(T) = \frac{\varepsilon_{pre}}{1 + c_f (T_g + \theta^{'} - T)^n} \cdot \left[(E_2 - E_r) \cdot \exp\left(-\left(\frac{T}{T_g} \right)^{m_2} \right) + E_r \right] \qquad (15)$$

To verify the applicability of the proposed model shown in equation (15), the numerical results of the model are plotted and compared with the experimental data [20] of the recovery stress with respect to temperature, for the MMA-co-PEGDMA polymer network with rubbery moduli of E_r =23 MPa and 17.2 MPa (both T_g =349K). The parameters used in equation (15) are shown in Table 4.

Table 4. Parameter values used in equation (15).

ε_{pre}	c_f	$\theta^{'}$ (K)	n	$E_2(MPa)(E_r = 23)$	$E_2(MPa)(E_r = 17.2)$	m_2
0.014	5.01e^{-6}	19	3.306	2000	1442,72	2

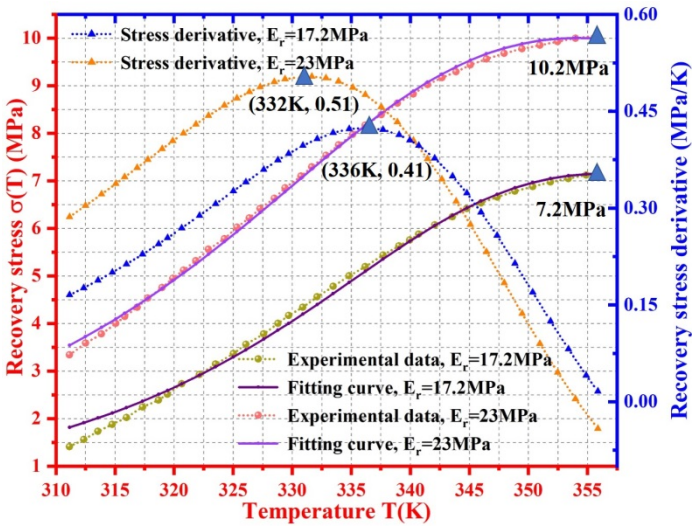

Figure 9. Comparisons between numerical results from equation (15) with the experimental data [20] for the recovery stress with respect to temperature, at a given T_g =349K and rubbery moduli of E_r =23 MPa and 17.2 MPa, and the corresponding stress derivative with temperature.

Figure 9 clearly shows that the simulation curves fit well with the experimental data. When the temperature is within the phase transition temperature region (e.g., from 310K to 355K), the recovery stress is dramatically increased with respect to temperature, and a larger recovery stress 10.2 MPa is achieved when the rubbery modulus of the SMP copolymer is 23MPa. From the numerical analysis of the derivative of the recovery stress as a function of temperature, this value is quite small when the temperature is over the glass transition temperature ($T_g = 349K$), which results in the insignificant changes of the recovery stress. The larger value of the recovery stress is obtained when the temperature is over the glass transition temperature. This indicates the significant release of the stored mechanical energy, which is critically determined by the rubbery modulus. The recovery stress can be significantly improved by means of increasing the rubbery modulus. Therefore, the

proposed model is useful to characterize and predict the mechanical recovery strength of the SMP copolymer.

From the above analysis, the largest value of the mechanical recovery stress is determined by the rubbery modulus. From equation (15), the recovery stress is also controlled by the glass transition temperature T_g. As illustrated in Figure (1) and Figure (2), both T_g and E_r are controlled by the molecular design (e.g., weight fraction of the PEGDMA (W_s) and molecular weight of PEGDMA monomer (M_n)). We further investigate the effects of two molecular design methods of the SMP copolymer on the tailorable recovery strength.

Firstly, the weight fraction of the PEGDMA is set as a constant ($W_s = 50\%$) but the molecular weight of the PEGDMA monomer is changed, e.g., $M_n = 400$, 500, 600 and 700 as shown in Figure 10(a). It is found that the lower value of the molecular weight of PEGDMA results in a higher value of T_g (from 338.4K at $M_n = 700$ to 381.6K at $M_n = 400$) and a higher value of recovery stress (from 33.6MPa at $M_n = 700$ to 57.8MPa at $M_n = 400$). This is mainly because of the increase of the degree of crosslinking in the SMP copolymer when the molecular weight of PEGDMA is decreased.

Next, we fix the molecular weight of the PEGDMA monomer as a constant ($M_n = 400$) and changed the weight fraction of the PEGDMA, e.g., $W_s = 20\%$, 40%, 60% and 80% as shown in Figure 10(b). Results show that although the glass transition temperature is decreased (e.g. from 401.2 K at $W_s = 20\%$ to 363.2 K at $W_s = 80\%$) with the increase of the weight fraction of PEGDMA in SMP copolymer,

the largest value of recovery stress is increased from 33.6 MPa at $W_s = 20\%$ to 56.9 MPa at $W_s = 80\%$.

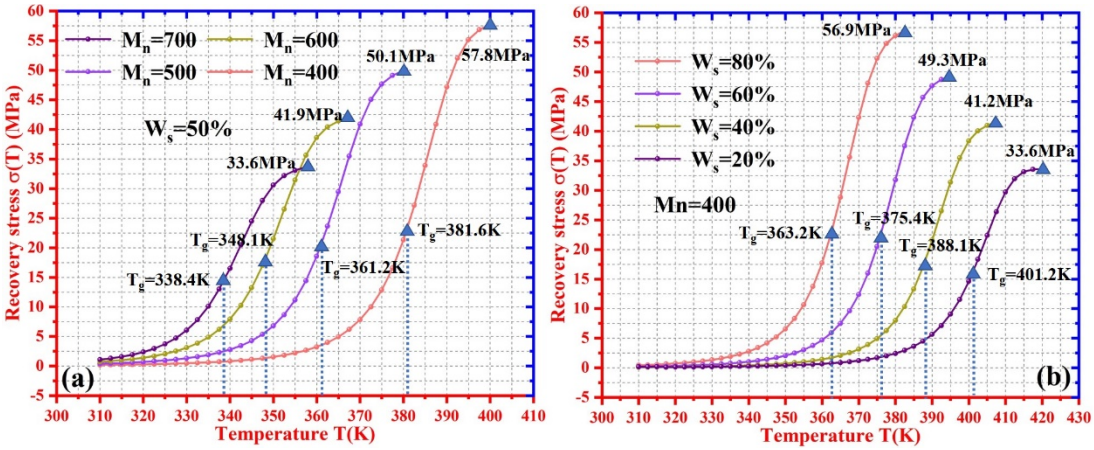

Figure 10. Theoretical analysis of influences of the weight fraction of PEGDMA (W_s) and molecular weight of PEGDMA monomer (M_n) on the recovery stress as a function of temperature. (a) M_n=400, 500, 600, 700 and W_s=50%, (b) W_s=20%, 40%, 60%, 80% and M_n=400.

Based on the above discussion, the recovery stress could be significantly changed when the SMP copolymer is in the rubbery state, and a larger value of recovery stress can be obtained with a lower value of the molecular weight of PEGDMA monomer and a higher value of the weight fraction of PEGDMA.

From the obtained recovery stress and strain, it is possible to characterize the stored mechanical energy (W), which is the driving force of the SME in shape memory polymers [42,43]. The stored mechanical energy can be obtained from the stress and strain parameters using the following equation:

$$W = \int \sigma(T) d\varepsilon = \frac{1}{2} E(T) \varepsilon^2 = \frac{1}{2} \left[(E_2 - E_r) \cdot \exp\left(-\left(\frac{T}{T_g} \right)^{m_2} \right) + E_r \right] \varepsilon^2 \qquad (16)$$

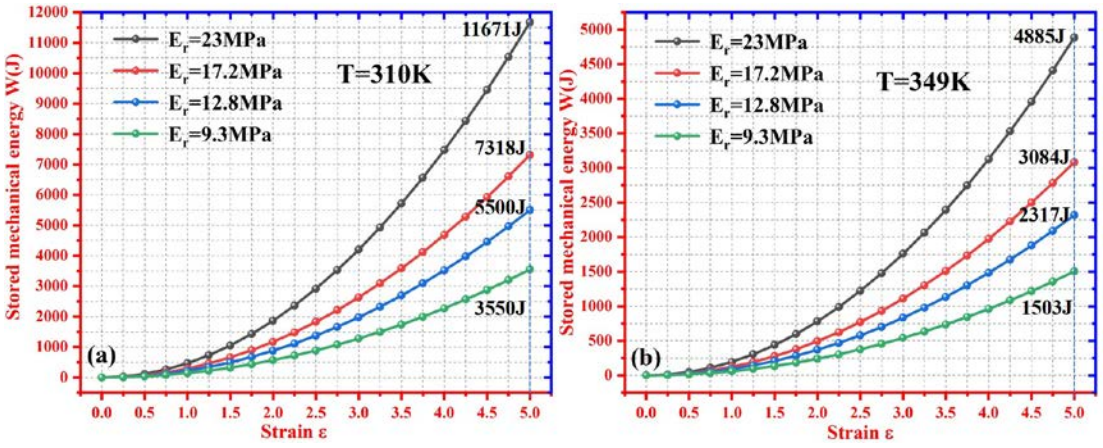

Figure 11. Theoretical analysis of influences of the rubbery modulus (E_r) and T_g on stored mechanical energy as a function of strain (ε). (a) T =310K and (b) T =349K.

Figure 11 presents the numerical results of stored mechanical energy obtained from the equation (17) at temperatures of T =310 K and 349 K, respectively. It is found that the stored mechanical energy is gradually increased with an increase in the strain. As shown in Figure 11(a), the stored mechanical energy is increased from 3550 J to 11671 J when the rubbery modulus is increased from 9.3 MPa to 23 MPa, at a given strain of ε =5.0 and T =310 K. Meanwhile, it is increased from 1503 J to 4885 J when the rubbery modulus is increased from 9.3 MPa to 23 MPa, at a given strain of ε =5.0 and T =349 K, as revealed in Figure 11(b). These simulation results clearly reveal that the higher rubbery modulus results in a higher stored mechanical energy. However, the stored mechanical energy is decreased from 11671 J to 4885 J with the temperature increased from 310 K to 349 K for the SMP copolymer, and in this case, the rubbery modulus is E_r =23 MPa and strain of ε =5.0. That is to say, a higher temperature results in a lower stored mechanical energy. As is well known, shape recovery of the SMP copolymer is a stress relaxation process, which is ruled by the Eyring equation below its T_g, but is ruled by the WLF equation above its T_g [30].

The relaxation time will be significantly shortened when the polymer is heated to a high temperature because the stored mechanical energy can be quickly released [19,30].

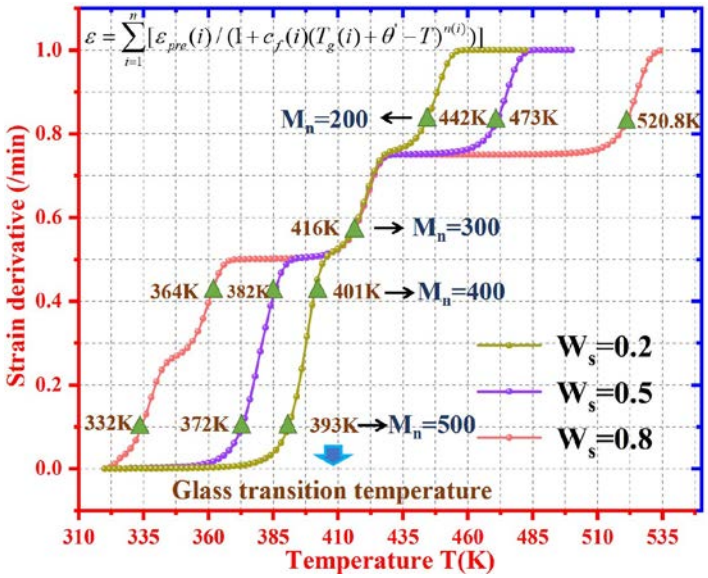

Figure 12. Theoretical analysis of the multi-SME in SMP copolymer by tuning the value of W_s and M_n of different segments.

As shown in equation (3), both weight fraction of the PEGDMA (W_s) and molecular weight of the PEGDMA monomer (M_n) have shown the significant effects on the glass transition temperature. A multiple glass transition process of SMP copolymers could be obtained by mixing different segments with different glass transition temperatures, which can be controlled by the value of W_s and M_n. Based on the Boltzmann's superposition principle and the series connection among different segments [33], the overall response of the recovery strain in multi-SMP copolymers are as follows,

$$\varepsilon = \sum_{i=1}^{n}[\varepsilon_{pre}(i)/(1+c_f(i)(T_g(i)+\theta^{'}-T)^{n(i)})] \quad (17)$$

where n is the number of transition segments, and subscript i represents the ith transition segments. The simulation results of the segmental relaxation behavior of multi-SMP copolymer are shown in Figure 12. The values of parameters used are listed in Table 1 and Table 4.

4. Conclusions

In this study, a phenomenological model was formulated to explore the working mechanism and describe the unique characteristics of the SMP copolymers with high mechanical recovery strengths and tailorable shape transition behavior. Fox-Flory equation and rubber elasticity theory were used to investigate the thermomechanical behaviors of SMP copolymers. Effects of the T_g, molecular weight and weight fraction of monomers on mechanical recovery strength were systematically studied. Based on the phase transition theory, effects of molecular structure characteristics on the shape transition behaviors were investigated. From the numerical analysis results using our proposed model, it can be concluded that this new model provides an effective design principle in the molecular scale which is favorable to achieve high mechanical recovery strength (i.e., elastic modulus, recovery stress and stored mechanical energy) and tailorable shape recovery behaviors of the SMP copolymers. Finally, experimental data have been employed to verify the proposed model, and the numerical results fit well with the experimental ones. This study is expected to provide an essential and effective tool to understand the working mechanism and provide a theoretical strategy for the design of SMP copolymers with high

mechanical recovery strength and tailorable shape transition behavior.

Acknowledgements

This work was financially supported by the National Natural Science Foundation of China (NSFC) under Grant No. 11672342 and 11725208, Newton Mobility Grant (IE161019) through Royal Society and the NSFC, and Royal academy of Engineering UK-Research Exchange with China and India.

Reference

(1) Hu, J.; Zhu, Y.; Huang, H.; Lu, J. Recent Advances in Shape-Memory Polymers: Structure, Mechanism, Functionality, Modeling and Applications. *Prog. Polym. Sci.* **2012**, 37 (12), 1720–1763.

(2) Zhang, H.; Wang, H.; Zhong, W.; Du, Q. A Novel Type of Shape Memory Polymer Blend and the Shape Memory Mechanism. *Polymer* **2009**, 50 (6), 1596–1601.

(3) Peterson, G. I.; Childers, E. P.; Li, H.; Dobrynin, A. V.; Becker, M. L. Tunable Shape Memory Polymers from α-Amino Acid-Based Poly(Ester Urea)S. *Macromolecules* **2017**, 50 (11), 4300–4308.

(4) Lu, H.; Yao, Y.; Huang, W. M.; Hui, D. Noncovalently Functionalized Carbon Fiber by Grafted Self-Assembled Graphene Oxide and the Synergistic Effect on Polymeric Shape Memory Nanocomposites. *Compos. Part B Eng.* **2014**, 67, 290–295.

(5) Lendlein, A.; Jiang, H.; Junger, O.; Langer, R. Light-induced shape-memory polymers. *Nature* **2005**, 434 (7035), 879-882.

(6) Mohr, R.; Kratz, K.; Weigel, T.; Lucka-Gabor, M.; Moneke, M.; Lendlein, A. Initiation of Shape-Memory Effect by Inductive Heating of Magnetic Nanoparticles in Thermoplastic Polymers. *Proc. Natl. Acad. Sci*. **2006**, 103 (10), 3540–3545.

(7) Koerner, H.; Price, G.; Pearce, N. A.; Alexander, M.; Vaia, R. A. Remotely Actuated Polymer Nanocomposites—Stress-Recovery of Carbon-Nanotube-Filled

Thermoplastic Elastomers. *Nat. Mater.* **2004**, 3 (2), 115–120.

(8) Hearon, K.; Wierzbicki, M. A.; Nash, L. D.; Landsman, T. L.; Laramy, C.; Lonnecker, A. T.; Gibbons, M. C.; Ur, S.; Cardinal, K. O.; Wilson, T. S.; et al. A Processable Shape Memory Polymer System for Biomedical Applications. *Adv. Healthc. Mater.* **2015**, 4 (9), 1386–1398.

(9) Yakacki, C. M.; Lyons, M. B.; Rech, B.; Gall, K.; Shandas, R. Cytotoxicity and Thermomechanical Behavior of Biomedical Shape-Memory Polymer Networks Post-Sterilization. *Biomed. Mater.* **2008**, 3 (1), 15010.

(10) Lei, M.; Hamel, C. M.; Yuan, C.; Lu, H.; Qi, H. J. 3D Printed Two-Dimensional Periodic Structures with Tailored in-Plane Dynamic Responses and Fracture Behaviors. *Compos. Sci. Technol.* **2018**, 159, 189–198.

(11) Jo, M. J.; Choi, H.; Kim, G. H.; Yu, W.-R.; Park, M.; Kim, Y.; Park, J. K.; Youk, J. H. Preparation of Epoxy Shape Memory Polymers for Deployable Space Structures Using Flexible Diamines. *Fibers Polym.* **2018**, 19 (9), 1799–1805.

(12) Wilson, S. A.; Jourdain, R. P. J.; Zhang, Q.; Dorey, R. A.; Bowen, C. R.; Willander, M.; Wahab, Q. U.; Willander, M.; Al-hilli, S. M.; Nur, O.; et al. New Materials for Micro-Scale Sensors and Actuators. An Engineering Review. *Mater. Sci. Eng. R Reports* **2007**, 56 (1–6), 1–129.

(13) Xie, T. Tunable Polymer Multi-Shape Memory Effect. *Nature* **2010**, 464 (7286), 267–270.

(14) Meng, H.; Li, G. A Review of Stimuli-Responsive Shape Memory Polymer Composites. *Polymer* **2013**, 54 (9), 2199–2221.

(15) Lu, H.; Wang, X.; Xing, Z.; Fu, Y.-Q. A Cooperative Domain Model for Multiple Phase Transitions and Complex Conformational Relaxations in Polymers with Shape Memory Effect. *J. Phys. D. Appl. Phys.* **2019**, 52 (24), 245301.

(16) Liu, C.; Qin, H.; Mather, P. T. Review of Progress in Shape-Memory Polymers. *J. Mater. Chem.* **2007**, 17 (16), 1543–1558.

(17) Mather, P. T.; Luo, X.; Rousseau, I. A. Shape Memory Polymer Research. *Annu. Rev. Mater. Res.* **2009**, 39 (1), 445–471.

(18) Ware, T.; Ellson, G.; Kwasnik, A.; Drewicz, S.; Gall, K.; Voit, W. Tough

Shape-Memory Polymer-Fiber Composites. *J. Reinf. Plast. Compos.* **2011**, 30 (5), 371–380.

(19) Fan, J.; Li, G. High Enthalpy Storage Thermoset Network with Giant Stress and Energy Output in Rubbery State. *Nat. Commun.* **2018**, 9 (1), 642.

(20) Yakacki, C. M.; Shandas, R.; Safranski, D.; Ortega, A. M.; Sassaman, K.; Gall, K. Strong, Tailored, Biocompatible Shape-Memory Polymer Networks. *Adv. Funct. Mater.* **2008**, 18 (16), 2428–2435.

(21) Smith, K. E.; Parks, S. S.; Hyjek, M. A.; Downey, S. E.; Gall, K. The Effect of the Glass Transition Temperature on the Toughness of Photopolymerizable (Meth)Acrylate Networks under Physiological Conditions. *Polymer* **2009**, 50 (21), 5112–5123.

(22) Ortega, A. M.; Kasprzak, S. E.; Yakacki, C. M.; Diani, J.; Greenberg, A. R.; Gall, K. Structure–property Relationships in Photopolymerizable Polymer Networks: Effect of Composition on the Crosslinked Structure and Resulting Thermomechanical Properties of a (Meth)Acrylate-based System. *J. Appl. Polym. Sci.* **2008** 110 (3), 1559-1572.

(23) Safranski, D. L.; Gall, K. Effect of Chemical Structure and Crosslinking Density on the Thermo-Mechanical Properties and Toughness of (Meth)Acrylate Shape Memory Polymer Networks. *Polymer* **2008**, 49 (20), 4446–4455.

(24) Li, Y.; Liu, Z. A Novel Constitutive Model of Shape Memory Polymers Combining Phase Transition and Viscoelasticity. *Polymer* **2018**, 143, 298–308.

(25) Pan, Z.; Zhou, Y.; Zhang, N.; Liu, Z. A Modified Phase-Based Constitutive Model for Shape Memory Polymers. *Polym. Int.* **2018**, 67 (12), 1677–1683.

(26) Li, Y.; Hu, J.; Liu, Z. A Constitutive Model of Shape Memory Polymers Based on Glass Transition and the Concept of Frozen Strain Release Rate. *Int. J. Solids Struct.* **2017**, 124, 252–263.

(27) Sujithra, R.; Srinivasan, S. M.; Arockiarajan, A. Modeling Memory Effects in Amorphous Polymers. *Int. J. Eng. Sci.* **2014**, 84, 95–112.

(28) Ge, Q.; Luo, X.; Iversen, C. B.; Mather, P. T.; Dunn, M. L.; Qi, H. J. Mechanisms of Triple-Shape Polymeric Composites Due to Dual Thermal Transitions. *Soft Matter*

2013, 9 (7), 2212–2223.

(29) Mao, Y.; Chen, F.; Hou, S.; Qi, H. J.; Yu, K. A Viscoelastic Model for Hydrothermally Activated Malleable Covalent Network Polymer and Its Application in Shape Memory Analysis. *J. Mech. Phys. Solids* **2019**, 127, 239-265.

(30) Yu, K.; Xie, T.; Leng, J.; Ding, Y.; Qi, H. J. Mechanisms of Multi-Shape Memory Effects and Associated Energy Release in Shape Memory Polymers. *Soft Matter* **2012**, 8 (20), 5687–5695.

(31) Fox, T. G.; Flory, P. J. Second-Order Transition Temperatures and Related Properties of Polystyrene. I. Influence of Molecular Weight. *J. Appl. Phys.* **1950**, 21 (6), 581–591.

(32) Gordon, M.; Taylor, J. S. Ideal Copolymers and the Second-Order Transitions of Synthetic Rubbers. I. Noncrystalline Copolymers. *Rubber Chem. Technol.* **2011**, 26 (2), 323–335.

(33) Ward, I. M.; Hadley, D. W. An Introduction to the Mechanical Properties of Solid Polymers. *John Wiley & Sons. LTD, New York.* **1993**.

(34) Richeton, J.; Schlatter, G.; Vecchio, K. S.; Rémond, Y.; Ahzi, S. A Unified Model for Stiffness Modulus of Amorphous Polymers across Transition Temperatures and Strain Rates. *Polymer* **2005**, 46 (19), 8194–8201.

(35) Liu, Y.; Gall, K.; Dunn, M. L.; Greenberg, A. R.; Diani, J. Thermomechanics of Shape Memory Polymers: Uniaxial Experiments and Constitutive Modeling. *Int. J. Plast.* **2006**, 22 (2), 279–313.

(36) Fan, H. B.; Yuen, M. M. F. Material Properties of the Cross-Linked Epoxy Resin Compound Predicted by Molecular Dynamics Simulation. *Polymer* **2007**, 48 (7), 2174 – 2178.

(37) Yang, Q.; Chen, X.; He, Z.; Lan, F.; Liu, H. The Glass Transition Temperature Measurements of Polyethylene: Determined by Using Molecular Dynamic Method. *RSC Adv.* **2016**, 6 (15), 12053 – 12060.

(38) Maple, J. O. N. R.; Dinurt, U. R. I.; Hagler, A. T. Derivation of Force Fields for Molecular Mechanics and Dynamics from Ab Initio Energy Surfaces. *Proc. Nati. Acad. Sci. USA* **1988**, 85, 5350–5354.

(39) Oie, T.; Maggiora, G. M.; Christoffersen, R. E.; Duchamp, D. J. Development of a Flexible Intra- and Intermolecular Empirical Potential Function for Large Molecular Systems. *Int. J. Quantum Chem.* **1981**, 20 (8), 1–47.

(40) Hockney, R. W.; Eastwood, J. W. Computer simulation using particles. *Taylor & Francis* **1988**.

(41) Steve, P. Fast Parallel Algorithms for Short-Range Molecular Dynamics. *J. Comput. Phys*. **1995**, 117 (1), 1–19.

(42) Yakacki, C. M.; Shandas, R.; Lanning, C.; Rech, B.; Eckstein, A.; Gall, K. Unconstrained Recovery Characterization of Shape-Memory Polymer Networks for Cardiovascular Applications. *Biomaterials* **2007**, 28 (14), 2255–2263.

(43) Meng, Q.; Hu, J. A Review of Shape Memory Polymer Composites and Blends. *Compos. Part A Appl. Sci. Manuf.* **2009**, 40 (11), 1661–1672.

Tables caption

Table 1. Parameter values used in equations (3) and (9).

Table 2. Experimental data of tBA-co-PEGDMA copolymers in Ref. [22].

Table 3. Parameter values used in equation (12).

Table 4. Parameter values used in equation (15).

Figures caption

Figure 1. Comparisons between numerical results using equation (3) and experimental data of the MMA-co-PEGDMA [20] at given molecular weights of PEGDMA monomer, e.g., M_n=330, 550, 750 and 1000.

Figure 2. Comparisons between results obtained from equation (9) and experimental data of the rubbery modulus as a function of W_s and M_n [20].

Figure 3. The molecular sketch map of the MMA, PEGDMA monomer, and the polymer system at the weight fraction of PEGDMA (W_s=20%， 40%， 60% and 80%), respectively.

Figure 4. Calculating the value of T_g from the intersections of the two linear fits to the glassy and rubbery regions at (a) W_s=20%; (b) W_s=40%; (c) W_s=60% and (d) W_s=80%.

Figure 5. Simulation results of T_g and E_r as a function of molecular weight (M_n) and weight fraction (W_s) of PEGDMA in SMP copolymer.

Figure 6. (a) Comparisons between simulation results and experimental data [22] of

the rubbery modulus as a function of weight fraction. (b) and (c) Comparisons between simulation results and experimental data of the storage modulus of the SMP copolymer with molecular weight of M_n=550 and M_n=750, respectively [22].

Figure 7. Comparisons between the numerical results obtained from equation (14) with experimental data [20] of the free recovery strain.

Figure 8. Numerical results of the normalized strain recovery as a function of temperature at a given weight fraction of W_s=0.8 (a) and (b) at a given molecular weight of M_n=500.

Figure 9. Comparisons between numerical results from equation (15) with the experimental data [20] for the recovery stress with respect to temperature, at a given T_g=349K and rubbery moduli of E_r=23MPa, 17.2MPa.

Figure 10. Theoretical analysis of influences of the weight fraction of PEGDMA (W_s) and molecular weight of PEGDMA monomer (M_n) on the recovery stress as a function of temperature. (a) M_n=400, 500, 600, 700 and W_s=50%, (b) W_s=20%, 40%, 60%, 80% and M_n=400.

Figure 11. Theoretical analysis of influences of the rubbery modulus (E_r) and T_g on stored mechanical energy as a function of strain (ε). (a) T=310K and (b) T=349K.

Figure 12. Theoretical analysis of the multi-SME in SMP copolymer by tuning the value of W_s and M_n of different segments.